

# Inhibition of acute leukemia with attenuated *Salmonella typhimurium* strain VNP20009

Meirong Li (✉ [mediali19851119@163.com](mailto:mediali19851119@163.com))

South China University of Technology

Mengmeng Lu

Guangdong University of Technology

Yunhao Lai

Guangdong University of Technology

Xindan Zhang

Guangdong University of Technology

Yuyu Li

Guangdong University of Technology

Ping Mao

Guangdong University of Technology

Zhicheng Liang

South China University of Technology

Yunping Mu

Guangdong University of Technology

Ying Lin

South China University of Technology

Allan Z. Zhao

Guangdong University of Technology

Zhenggang Zhao

Guangdong University of Technology

Sujing Zhou

Guangdong University of Technology

Fanghong Li

Guangdong University of Technology

---

## Research

**Keywords:** acute leukemia, attenuated *Salmonella typhimurium* VNP20009, immunotherapy, bacterial cancer therapy, apoptosis

**Posted Date:** April 7th, 2020

**DOI:** <https://doi.org/10.21203/rs.3.rs-20815/v1>

**License:**  This work is licensed under a Creative Commons Attribution 4.0 International License.

[Read Full License](#)

---

**Version of Record:** A version of this preprint was published at Biomedicine & Pharmacotherapy on September 1st, 2020. See the published version at <https://doi.org/10.1016/j.biopha.2020.110425>.

# Abstract

**Background** Despite recent promising progress, the prognosis of acute leukemia (AL) patients remains to be improved. New therapies are therefore still needed. Spontaneous complete remission (SCR) of leukemia caused by severe bacterial infection in clinic suggests the possibility of bacterial treatment for AL. An engineered attenuated *Salmonella typhimurium* VNP20009 with good tolerance and safety has been shown to be highly effective as an anti-tumor agent in many solid cancer models, but it has not been applied in leukemia. Therefore, we selected VNP20009 as a candidate for the bacterial therapy of AL in this study.

**Methods** Murine xenograft tumor models were used to verify the growth inhibition effect of VNP20009 on AL tumors. Histopathological features of the tumor were observed by H&E staining, Ki-67 immunohistochemical staining and TUNEL immunofluorescence staining. The apoptosis proteins Bax and cleaved caspase-3 in tumors were detected by Western blotting. The ratios of apoptosis, green fluorescent protein positive (GFP + ) cells and immune cells were detected by flow cytometry. Blood cell count were counted by IDEXX automatic five-classification blood cell analyzer. Detection of cytokines and chemokines in serum was completed on a Luminex Multi-factor Detection Platform.

**Results** VNP20009 can induce apoptosis of AL cells by up-regulating the expression levels of Bax and cleaved caspase-3 . Furthermore, VNP20009 significantly inhibited the proliferation of MLL-AF9-induced AML cells and prolonged the survival of the AML-carrying mice. VNP20009 restored the counts of white blood cell and its five subsets in PB to near-physiological values, and elevated the levels of certain cytokines, such as tumor necrosis factor- $\alpha$  (TNF- $\alpha$ ), leukemia inhibitory factor (LIF), interferon- $\gamma$  (IFN- $\gamma$ ), chemokine C-X-C motif ligand-10 (CXCL-10) and C-C motif ligand-2 (CCL-2). Moreover, the ratio of immune cells, including natural killer cells (NKs), CD4 + Th1-type cells and CD8 + IFN- $\gamma$ -producing effector T cells were highly upregulated in the AML mice treated with VNP20009.

**Conclusions** VNP20009 induces the apoptosis of AL cells and activates the immune system, leading to the development of a strong and effective anti-tumor systemic response and tumor remission in acute leukemia. **Keywords:** acute leukemia, attenuated *Salmonella typhimurium* VNP20009, immunotherapy, bacterial cancer therapy, apoptosis

## Background

Acute leukemia is a common hematological malignancy that includes acute myelocytic leukemia (AML) and acute lymphoblastic leukemia (ALL) [1]. Of these, ALL involving the abnormal proliferation of lymphocytes, is the most common malignancy. Both subtypes can progress rapidly but differ considerably in terms of survival (5 year survival: 67.5% and 25.9% for ALL and AML, respectively) [2]. To date, chemotherapy is still the main treatment strategy for leukemia. Hematopoietic stem cell transplantation is usually considered when the chemotherapy fails or leukemia relapses, but demands a stringent matching requirement for the donors [3]. Thus, new target and pharmaceutical approach are still

sorely needed for acute leukemia. Since acute leukemia often evades immune recognition and destruction by cytotoxic T lymphocytes by a variety of mechanisms [4], augmentation of innate anti-tumor immunity has become a highly promising approach to treat acute leukemia.

The use of bacteria for the development of immunotherapies for cancer has great potential. Bacteria are potent natural adjuvants that can activate anti-tumor immunity by interacting with innate immune cells. It induces the secretion of tumor necrosis factor- $\alpha$  (TNF- $\alpha$ ), interferon- $\gamma$  (IFN- $\gamma$ ), interleukin-12 (IL-12), and other inflammatory mediators [5]. These cytokine signals amplify the early innate anti-tumor responses through the recruitment and activation of dendritic cells (DCs) that migrate to the draining lymph nodes and present tumor antigens, effectively priming anti-tumor effector T cells [6]. The first bacterial product for cancer immunotherapy was developed by William Coley more than a century ago [7, 8]. The past few decades have witnessed the development of bacterial anti-tumor therapy, including the utilization of various bacteria, such as *Salmonella*, *Clostridium* and *Escherichia coli* [9, 10]. Among all the anti-tumor bacterial species, *Salmonella* has been the most studied. In addition to its excellent tumor targeting and colonization ability [11], *Salmonella* can also activate both the innate and adaptive immune responses against tumors, which has a natural selection advantage in the anti-tumor bacterial therapy [10].

Using natural bacteria in fighting cancer runs the risk of high toxicity and sepsis, which in turn limits its clinical use. Previous research using genetic engineering created a *Salmonella* strain, VNP20009, with a null mutation in *msbB* gene [12], which leads to greatly reduced production of endotoxin. Such attenuated *Salmonella* strain has been shown to possess specific targeting and anti-tumor effects to a broad range of solid tumors in mice or spontaneous canine tumors, including melanoma, lung, colon, breast, renal, hepatic tumors [9, 10, 13–16]. Importantly, its tolerance and safety have been proven in patients in a phase I clinical trial [17, 18]. However, the application of such attenuated *Salmonella* in the treatment of acute leukemia remains to be explored.

Given the excellent safety profile of VNP20009, we aim to evaluate the therapeutic effects of VNP20009 on acute leukemia, particularly in T-cell acute lymphoblastic leukemia (T-ALL) and AML models. The potential therapeutic value of this approach, in promoting local and systemic immunity against acute leukemia, may merit translation into future clinical trials.

## Materials And Methods

### Cells and culture conditions

Murine T-ALL cell line L1210 (ATCC® CCL-219™) cultured in Dulbecco's modified Eagle's medium (DMEM; Gibco) supplemented with 10% fetal bovine serum (FBS; Gibco). Human acute promyelocytic leukemia (a subtype of AML) cell line HL-60 (ATCC® CCL-240™) cultured in Iscove's Modified Dubecco's Medium (IMDM; Gibco) supplemented with 20% FBS. Human T-ALL cell line Jurkat, Clone E6-1 (ATCC® TIB-152™) cultured in Roswell Park Memorial Institute 1640 (RPMI 1640; Gibco) supplemented with 10% FBS. All cell lines were purchased from and maintained in a 37 °C incubator with 5% CO<sub>2</sub>.

## Bacterial strain

Attenuated *Salmonella typhimurium* VNP20009 (ATCC 202165) was grown in modified Luria-Bertani (LB) broth containing 1% tryptone, 0.5% yeast extract, 1 mM CaCl<sub>2</sub>, and 1 mM MgSO<sub>4</sub>, pH 7.0-7.2.

## Mice

Five-week-old female athymic Balb/c nu/nu mice and seven-week-old male C57BL/6 mice were purchased from the Model Animal Research Center of Nanjing University. All mice were maintained in an SPF environment in strict accordance with the animal care guidelines of the Laboratory Animal Centre of Guangdong Pharmaceutical University.

## Apoptosis assay

Leukemia cells were seeded in 6-well plates to a density of approximately  $1 \times 10^5$  cells per well. VNP20009 were added to the tumor cells at a multiplicity of infection 100:1 with no bacteria addition as the negative control. Cell culture plates were incubated at 37 °C in a 5% CO<sub>2</sub> atmosphere for 30 minutes before addition of 50 µg/mL gentamycin and 50 µg/mL penicillin to the culture. The treated cells were cultured for another 48 hours before the detection of apoptosis using flow cytometry with Annexin V-PE/7-amino-actinomycin (7-AAD) Apoptosis Detection Kit (BD, 559763) according to manufacturer's instructions.

## Subcutaneous xenograft model and bacterial application

L1210 cells ( $1 \times 10^5$ ) or HL-60 cells ( $5 \times 10^6$ ) were inoculated subcutaneously into the right flank of athymic Balb/c nu/nu mice. When tumor volumes reached to the size of approximately 80–100 mm<sup>3</sup>, mice received a single intratumoral injection of PBS (20 µL) or VNP20009 ( $2 \times 10^6$  CFU/20 µL). Tumor length and width were measured every 2 or 3 days, and tumor volumes were calculated according to the formula: Tumor volume = width<sup>2</sup> × length × 0.5 (mm<sup>3</sup>). Relative tumor volume growth (% of V<sub>0</sub>) = tumor volume/initial therapeutic volume (V<sub>0</sub>).

## MLL-AF9-induced acute myeloid leukemia mouse model

Liquid nitrogen preserves murine AML primary marrow cells with a report green fluorescent protein (GFP) initiated by human MLL-AF9 fusion protein [19] were kindly provided by Professor Cheng Tao from State Key Laboratory of Experimental Hematology, Tianjin, China.  $1.5 \times 10^6$  murine AML (GFP<sup>+</sup>) primary marrow cells were transplanted into C57BL/6 mice via tail vein injection. The next day after mouse AML bone marrow cells were transplanted, mice received one (on day 1) or two (on day 1 and day 8) tail vein injections of PBS or VNP20009 ( $2 \times 10^6$  CFU/mouse, one dose: V1, two doses: V2).

## Histology and immunohistochemistry

Tumors were fixed with neutral fixative, embedded in paraffin, and cut into 4 µm sections. The sections were stained with hematoxylin and eosin (H&E). Immunohistochemistry (IHC) was performed on paraffin

sections using anti-Ki-67 antibody (CST, #12202). Images were taken with a Leica microscope.

## **TUNEL assay**

Terminal deoxynucleotidyl transferase (TdT)-mediated dUTP nick end labeling (TUNEL) assay was performed on tumor paraffin sections with a TUNEL Bright Red Apoptosis Detection Kit (Vazyme, A113) according to the manufacturer's instructions. Images were taken with a Leica fluorescent microscope.

## **Western blot**

Tumor tissues were homogenized and lysed in RIPA buffer (Beyotime, P0013B) containing 1 mM PMSF and then processed with ultrasonic probe and subsequent centrifugation to obtain protein extract. Total protein concentration was measured with a BCA assay kit (Thermo Fisher, 23225). Total cell lysates were separated by SDS-PAGE (12% separation gel and 5% concentrated gel) and transferred to nitrocellulose, followed by blocking in 5% (vol/vol) milk in TBST, probing with the indicated antibodies and visualization by chemiluminescence (Thermo Fisher, 1863096 & 1863097). All primary antibody dilutions were at 1:1000, and secondary antibody dilutions were at 1:5000. The primary antibodies were rabbit anti-Bax antibody (CST, #2772), rabbit anti-Cleaved-caspase-3 antibody (CST, #9661) and mouse anti- $\beta$ -actin antibody (Sigma Aldrich, A5316). The secondary antibodies were goat anti-rabbit IgG (Jackson lab, 111-035-003) and goat anti-mouse IgG (Jackson lab, 115-035-003).

## **Blood cell count**

White blood cells (WBCs), red blood cells (RBCs), platelets (PLTs) and five WBC subsets in peripheral blood (PB) of mice were counted by IDEXX automatic five-classification blood cell analyzer according to the manufacturer's instructions.

### Measurement of cytokines and chemokines

The detection of cytokines and chemokines in serum was entrusted to the laboratory of Univ-bio Company (Shanghai) and completed on a Luminex Multi-factor Detection Platform.

## **Flow cytometric analysis**

Mouse blood samples and splenocytes were obtained, and erythrocytes were lysed. AML (GFP<sup>+</sup>) cells were detected directly by flow cytometry in an FITC channel gated on WBCs. The following anti-mouse surface antibodies CD3-PE (145-2C11; BD, 553063), CD4-APC (RM4; BD, 553051), CD8-PercpCy5.5 (53-6.7; BD, 561109), and NK1.1-APC (PK126; BD, 561117) were used for extracellular FACS, the anti-mouse antibody IFN- $\gamma$ -PECy7 (XMG1.2; BD, 557649) was used for intracellular FACS. Nonspecific surface molecules were blocked with mouse Fc Block (BD, 553141) prior to cell surface markers staining. For intracellular cytokine FACS, we stimulated cells with PMA (50 ng/mL; Sigma-Aldrich, P1585), ionomycin (1  $\mu$ M; Sigma-Aldrich, 407953), and brefeldin A (5  $\mu$ g/mL; Sigma-Aldrich, 203729) for 5 hours. Cells were fixed and permeabilized with Fixation/Permeabilization Solution (BD, 555028) and then stained for IFN- $\gamma$ . The FSC and SSC plots were used to distinguish lymphocytes. The detection of natural killer cells (NK cells) and CD3<sup>+</sup> T cells gated on whole GFP<sup>-</sup> lymphocytes; CD4<sup>+</sup>, CD8<sup>+</sup> and  $\gamma\delta$ T cells (CD3<sup>+</sup>CD4<sup>-</sup>CD8<sup>-</sup>

cells) gated on CD3<sup>+</sup> T cells. Their percentages in lymphocytes were calculated finally. The data were analyzed using FlowJo 10.0 software.

## Statistical analysis

Statistical analyses and graphs were performed using GraphPad Prism 7.0 (GraphPad Software Inc., CA, USA). Data are shown as means  $\pm$  SEM. Two-tailed unpaired Student's t test or one-way analysis of variance test was used, followed by Tukey's test, unless otherwise stated in the figure legends. A result of  $P < 0.05$  was considered to be statistically significant.

## Results

### Induction of apoptosis of acute leukemia cells by VNP20009 treatment *in vitro*

To test whether VNP20009 could directly induce apoptosis in acute leukemia cells, we conducted co-culture experiments with VNP20009 and L1210 (murine T-ALL), Jurkat (human T-ALL), HL-60 (human AML) cell lines. Approximately 48 h post-infection, the apoptotic rates in the cells were significantly higher than those in non-infected cells (Fig. 1), indicating that VNP20009 could directly cause cell death in acute leukemia cells by inducing apoptosis with varying rates of cell death in different acute leukemia cell lines.

### VNP20009 suppresses the growth of murine T-cell acute lymphoblastic leukemia model

To evaluate the potential of VNP20009 against leukemia growth *in vivo*, we established a subcutaneous tumor model with the murine T-ALL cells L1210. After tumor establishment, the mice received a single intratumoral injection of PBS or VNP20009. VNP20009 delivery led to a significant retardation of L1210 tumor growth compared with the PBS-treated group (Fig. 2A), but did not cause any significant changes in body weight or any adverse behavioral effects relative to the PBS control group (Fig. S1A). The relative tumor volume growth (% of  $V_0$  (right before treatment)) in the VNP20009-treated group was 207.7% and 455.3% on days 2 and 5, compared with 784.5% and 1,706% in the PBS-treated group, respectively (Fig. 2B). The final average tumor/body weight ratios were 4.353% and 2.833% in the PBS and VNP20009 treated groups by the end of the treatment, respectively (Fig. 2C and 2D). Hematoxylin and eosin (H&E) staining revealed that the tumor tissues in the VNP20009-treated group exhibited large areas of necrosis, nuclear fragmentation, incomplete cell membranes, and loss of normal morphology (Fig. 2E). Moreover, Ki-67 (a marker of proliferation) staining showed light or no staining in the corresponding necrotic areas (Fig. 2F) and TUNEL (a marker of apoptosis) staining showed positive results in the necrotic areas (Fig. 2G). Western blot analysis showed a significant increase in the expression of Bax protein and the cleaved form of caspase-3 (Fig. 2H, 2I and S3), indicating that VNP20009 induced apoptosis in L1210 tumors. Taken together, these data showed that VNP20009 exerted strong inhibitory effect on the growth of murine T-ALL.

# VNP20009 suppresses the growth of human acute promyelocytic leukemia xenografts

We wondered if VNP20009 could have similar therapeutic impact on human AML. To this end, we deployed a subcutaneous xenograft of human acute promyelocytic leukemia cell line, HL-60, in the Balb/c nu/nu mice. After tumor establishment, the mice underwent the same treatment procedure as those performed in the L1210 tumor model. Tumor growth was sharply inhibited by VNP20009 treatment without causing significant loss of body weights (Fig. 3A-3D and S1B). Again, VNP20009 caused large necrotic areas, loose and disorganized structures, and the necrosis was even more profound than that observed in the L1210 tumor model (Fig. 3E). Similarly, large portion of negative Ki-67 staining and positive TUNEL staining were evident in the necrotic areas (Fig. 3F and 3G) in VNP20009 treated group. Significant elevation in Bax protein expression and the cleaved caspase-3 activity (Fig. 3H, 3I and S4) were also consistent with the observations in the L1210 tumor model described above. These results showed that VNP20009 treatment potently inhibited the growth of not only murine T-ALL but also acute promyelocytic leukemia xenograft in mice.

## VNP20009 treatment prolongs the survival in MLL-AF9 induced AML model

To further study the therapeutic impact of VNP20009 on acute leukemia and the interplay between VNP20009 and the immune system, we used an AML mouse model that was derived from MLL-AF9 cells [19]. Such model has been well established in mimicking the development of human AML [19]. The established MLL-AF9 leukemia cells, positive for green-fluorescent protein (GFP) and myeloid lineage markers, were transplanted into immunocompetent mice before given either one or two intravenous injections of VNP20009 with a dose of  $2 \times 10^6$  CFU/injection/mouse (Fig. 4A). Flow cytometry analysis showed that the percentage of GFP<sup>+</sup> AML cells in the white blood cells (WBCs) of peripheral blood (PB) increased rapidly during leukemia development on day 7, 14, and 20 (Fig. 4B and 4C). Both the single injection and the double injections significantly inhibited the proliferation of AML cells with the double injections generating stronger inhibitory effect than that of a single dose (Fig. 4D). On day 14 after AML establishment, the proportion of GFP<sup>+</sup> AML cells in the spleen was significantly lower in VNP20009-treated group than that in the PBS group (Fig. 4E and 4F) and the inhibition rate was 82.82% (Fig. 4G). All treated mice did not exhibit any significant loss in body weight during the entire observation period (Fig. S1C). The survival duration of the mice that received two intravenous injections of VNP20009 was significantly longer than those of PBS or single dose-treated mice (Fig. 4H). Thus, VNP20009 could inhibit the proliferation of leukemia cells in the peripheral blood and spleen of AML mice.

### VNP20009 restores the counts of WBCs and its subtypes to near-normal levels in the AML mice

On day 14 after AML establishment, the mice exhibited elevated counts of WBCs which was consistent with the symptoms of AML ( $P < 0.001$ ) (Fig. 5A). Two injections of VNP20009 treatment also reduced red

blood cell (RBC) counts (Fig. 5B) as well as PLT counts (Fig. 5C), indicating, to some extent, the possibility of anemia. The treatment with the bacteria reduced WBC counts and leukocytes subsets, including lymphocytes (LYMPH), monocyte (MONO), neutrophil (NEUT), and eosinophil (EO) to near-physiological levels in the AML mice ( $P < 0.001$ ) (Fig. 5A, 5D-5G), while the basophil (BASO) counts were hardly affected ( $P < 0.001$ ) (Fig. 5H). Combined together, hematology results revealed VNP20009 did not cause any severe toxicological damage. In contrast, it could inhibit the malignant proliferation of multi-lineage subsets of WBCs in AML mice.

## **Cytokines and chemokines in the VNP20009-treated AML mice**

We measured a number of cytokines and chemokines on day 14 in PBS- and VNP20009-treated AML mice (with two injections). Our results showed that in the VNP20009-treated mice, serum levels of IFN- $\gamma$ , TNF- $\alpha$ , LIF, Chemokine C-X-C motif ligand-10 (CXCL-10) and C-C motif ligand-2 (CCL-2) were significantly increased (Fig. 5I-5M). In contrast, the levels of GM-CSF (Granulocyte-macrophage colony stimulating factor) were significantly decreased compared with PBS-treated mice (Fig. 5N). Thus, VNP20009 can exert the therapeutic action on acute leukemia potentially by modulating the expression of multiple cytokines and chemokines, thereby strengthening the native anti-leukemia immunity in the AML mice.

## **VNP20009 stimulates the native and adaptive immune cells in PB and spleen of AML mice**

We applied flow cytometry to analyze the response of natural killer cells (NK cells), the front line of immune defense against infection and tumor, in the AML mouse models. The proportion of NK cells in the VNP20009 treated group was significantly higher than that in the control group on day 14 both in PB and spleen (Fig. 6A and 6B). In the analysis of the adaptive immunity, we found that the proportion of CD3<sup>+</sup> T cells in VNP20009 treated group was higher than that in the control on day 7, 14, and 20 in PB samples (Fig. 76C and 6D). The increase of CD3<sup>+</sup> T cells was dominated by the increase of CD4<sup>+</sup> T cells, while the percentages of CD8<sup>+</sup> T cells and  $\gamma\delta$ T (CD3<sup>+</sup>CD4<sup>-</sup>CD8<sup>-</sup>) cells showed no ostensible changes (Fig. 6C and 6D). In the spleen samples, the levels of CD3<sup>+</sup>, CD4<sup>+</sup>, CD8<sup>+</sup> and  $\gamma\delta$ T cells were consistent with those observed in the blood samples of the treated AML mice (Fig. 6C and 6E). Within the T-cell population associated with tumor immunity, the proportion of Th1-subtype, CD4<sup>+</sup>IFN- $\gamma$ <sup>+</sup>, and the CD8-subtype, CD8<sup>+</sup>IFN- $\gamma$ <sup>+</sup>, showed remarkable increase on day 14 in the spleens of VNP20009 treated AML mice (Fig. 6F and 6G). These observations, evaluated as a whole, suggested that VNP20009 treatment activated the native and adaptive immunity, thereby boosted anti-tumor activity.

## **Discussion**

Spontaneous complete remission (SCR) of leukemia denotes either partial or complete morphologic disappearance of leukemia without administration of anti-leukemic therapy. The earliest report of SCR in AML was published in 1878 and subsequent publications have reported about 100 cases of SCR in acute

leukemia worldwide [20, 21]. Most SCRs have been reported to be accompanied by severe microbial infection. In patients with SCR, the serum levels of tumor TNF- $\alpha$ , IFN- $\gamma$ , the cell counts of CD4<sup>+</sup> or CD8<sup>+</sup> cytotoxic T lymphocyte cells (CTLs) and NK cells were increased [22, 23]. Persistent infection provokes strong and sustained activation of immune response is important to complete tumor regression [7, 8]. However, using natural bacteria to fight leukemia runs the risk of sepsis. In this study, we have chosen a previously engineered and well-characterized attenuated *Salmonella* typhimurium strain, VNP20009, as the treatment agent of acute leukemia. The combined results revealed that intravenous delivery of VNP20009 led to innate and adaptive immune response in acute leukemia mice, hindered leukemia proliferation and provoked leukemia cell apoptosis both *in vitro* and *in vivo*. To our knowledge, this represents the first report to show that *Salmonella* can cause significant regression of acute leukemia.

Bacteria naturally have a therapeutic effect on tumors [11] [24]. Native toxicity of bacteria can specifically bind to target cells and regulate the proliferation and apoptosis of human leukemia cells without causing damages to other non-leukemic cells [25, 26]. In our study, VNP20009 could directly induce apoptosis in co-culture experiments with leukemia cells *in vitro*, inhibit tumor growth, and cause tumor regression in the subcutaneous tumor model. We also saw elevated expression of apoptosis-promoting protein, Bax and cleaved caspase-3, implying that the killing of leukemia cells was mediated at least in part through the mitochondrial apoptosis pathway. Such result is also consistent with our previously study that VNP20009 could induce apoptosis in CFPAC-1 pancreatic cancer by increasing bax and cleave-caspase-3 protein expression [16]. In a well-established blood model of AML derived from the MLL-AF9 cells, either one or two intravenous injections of VNP20009 could retard the proliferation of AML cells, albeit only the double injections of VNP20009 prolonged the survival of the AML mice. Clinical observations, body weight and hematology results revealed VNP20009 bacteria were well tolerated by the acute leukemia-bearing mice. Thus, the attenuated *Salmonella* bacterium, VNP20009 could inhibit the proliferation and induce the apoptosis of acute leukemia cells without causing any severe toxicological damage.

*Salmonella* can also sensitize the host immune system [10], which serves as part of the mechanisms contributing to the efficacy of VNP20009 in treating hematologic malignancies. We found that VNP20009 treatment led to significantly elevated blood levels of proinflammatory cytokines (IFN- $\gamma$ , TNF- $\alpha$ ) and chemokines (CXCL-10, CCL-2) in acute leukemia mice, which in turn could recruit a variety of immune cells to participate in the immune response and enhance anti-tumor immunity [5]. CCL-2 is a primary chemoattractant for T lymphocytes, monocytes, macrophages, mast cells, and endothelial cells [27, 28]. CXCL-10, induced by IFN- $\gamma$ , also induces chemotaxis of various subtypes of leukocytes, including T and B lymphocytes, NK cells, DCs, and macrophages [29]. Thus, part of the mechanisms for the attenuated *Salmonella* to induce the killing of leukemia cells is likely mediated by promoting inflammatory cytokines that leads to recruitment of various immune cells to the leukemia cells.

We found that the percentage of NK cells were significantly increased in the blood or spleen samples of VNP20009 treated-AML mice. NK cells participate in the first natural defense immunity against infection and tumor, and play crucial roles in tumor surveillance [30]. VNP20009 treatment also promoted proliferation of CD3<sup>+</sup> T lymphocytes in both blood and spleens of AML mice. Subset analysis of these T

cells showed that they were dominated by CD4<sup>+</sup> T cells after treatment. In addition, VNP20009 treatment was associated with significantly higher ratio of Th1 cells of CD4<sup>+</sup>IFN- $\gamma$ <sup>+</sup> and CTLs of CD8<sup>+</sup>IFN- $\gamma$ <sup>+</sup> in the spleen of AML mice. CD4<sup>+</sup> T cells can further differentiate into Th1 cells to directly kill tumor cells by IFN- $\gamma$  mediated mechanism and activating CD8<sup>+</sup> T to differentiate into cytotoxic T-cells that also secrete IFN- $\gamma$  and TNF- $\alpha$  to maintain and enhance the anti-tumor response [31]. Consistent with our observations, previous report has shown that *Salmonella* could promote tumor killing effects via Th1-type immune response and neutrophil activation in a mouse model of breast cancer [32].

## Conclusion

As shown in the graphic summary of this study (**Fig. S2**), the attenuated strain of *Salmonella*, VNP20009, induces the apoptosis of acute leukemia cells and activates the immune system, leading to the development of a strong and effective anti-tumor systemic response and tumor remission in acute leukemia. It may be applied as a stand alone or in combination with other therapies, to better treat acute leukemia or other hematologic malignancies.

## Abbreviations

### **AL**

Acute leukemia

### **AML**

Acute myelocytic leukemia

### **ALL**

Acute lymphoblastic leukemia

### **T-ALL**

T-cell acute lymphoblastic leukemia

### **TNF- $\alpha$**

Tumor necrosis factor- $\alpha$

### **IFN- $\gamma$**

Interferon- $\gamma$

### **IL-12**

Interleukin-12

### **DCs**

Dendritic cells

### **NK cells**

Natural killer cells

### **SCR**

Spontaneous complete remission

### **IMDM**

Iscoe's Modified Dubecco's Medium

**RPMI 1640**

Roswell Park Memorial Institute 1640

**DMEM**

Dulbecco's modified Eagle's medium

**LB**

Luria-Bertani

**7-AAD**

Annexin V-PE/7-amino-actinomycin

**GFP**

Green fluorescent protein

**H&E**

Hematoxylin and eosin

**IHC**

Immunohistochemistry

**TUNEL**

Terminal deoxynucleotidyl transferase (TdT)-mediated dUTP nick end labeling

**WBCs**

White blood cells

**RBCs**

Red blood cells

**PLTs**

Platelets

**PB**

Peripheral blood

**LYMPH**

Lymphocytes

**MONO**

Monocyte

**EO**

Eosinophil

**NEUT**

Neutrophil

**BASO**

Basophil

**CCL-2**

C-C motif ligand-2

**CCXC-10**

Chemokine C-X-C motif ligand-10

**IFN- $\gamma$** 

Interferon- $\gamma$

**LIF**

Leukemia inhibitory factor

**GM-CSF**

Granulocyte-macrophage colony stimulating factor

**CTLs**

Cytotoxic T lymphocyte cells

## Declarations

**Ethics approval and consent to participate**

Ethics approval and consent to participate. All animal experiments were approved by the Animal Care Committee of Guangdong Pharmaceutical University.

**Consent for publication**

All authors have agreed to publish this manuscript.

**Availability of data and materials**

Please contact author for data requests.

**Competing interests**

The authors declare that they have no competing interests in this study.

**Funding**

This work was supported by grants from the National Key R&D Program of China (2018YFA0800600 to AZZ); the National Natural Science Foundation of China (81630021 to AZZ); Key research and development program of Guangdong Province for "Innovative drug creation" (2019B020201015 to FHL); the Guangdong Innovative Research Team Program (2016ZT06Y432 to AZZ, FHL and SJZ); the National Program on Key Basic Research Project of China (2013CB945202 to AZZ and FHL); and the Startup R&D Funding of Guangdong University of Technology (50010102 to AZZ and FHL).

**Authors' Contributions**

Allan Z. Zhao and Fanghong Li proposed research concept. Meirong Li, Zhenggang Zhao and Sujin Zhou designed the research projects. Meirong Li, Xindan Zhang, Yuyu Li and Ping Mao carried out the experiments. Mengmeng Lu, Yunhao Lai, Zhicheng Liang and Yunping Mu provided technical guidance. Meirong Li and Zhenggang Zhao analyzed the experimental data. Meirong Li wrote and revised the manuscript under the directions of Ying Lin, Allan Z. Zhao, Zhenggang Zhao, Sujin Zhou and Fanghong Li. All authors read and approved the final manuscript.

## Acknowledgment

We would like to thank Professor Tao Cheng and Dr. Shihui Ma from State Key Laboratory of Experimental Hematology, Tianjin, China for providing the MLL-AF9-induced acute myeloid leukemia cells and technical assistance.

## Authors' information

### Affiliations

*School of Biological Science and Engineering, South China University of Technology, Guangzhou, Guangdong, China*

Meirong Li, Ying Lin

*School of Biomedical and Pharmaceutical Sciences, Guangdong University of Technology, Guangzhou, Guangdong, China*

Mengmeng Lu, Yunhao Lai, Xindan Zhang, Yuyu Li, Ping Mao, Yunping Mu, Allan Z. Zhao, Zhenggang Zhao, Sujin Zhou, Fanghong Li

*School of Medicine, South China University of technology, Guangzhou, Guangdong, China*

Zhicheng Liang

Corresponding author

Correspondence to Zhenggang Zhao, Sujin Zhou and Fanghong Li.

## References

1. Miranda-Filho A, Pineros M, Ferlay J, Soerjomataram I, Monnereau A, Bray F. Epidemiological patterns of leukaemia in 184 countries: a population-based study. *Lancet Haematol.* 2018;5(1):e14–24.
2. Bispo JAB, Pinheiro PS, Kobetz EK. *Epidemiology and Etiology of Leukemia and Lymphoma.* Cold Spring Harb Perspect Med. 2019.
3. Liso A, Neri M, Maglietta F, La Russa R, Turillazzi E. Hematopoietic Stem Cell Transplantation: A Bioethical Lens. *Stem Cells Int.* 2017;2017:1286246.

4. Knaus HA, Kanakry CG, Luznik L, Gojo I. Immunomodulatory Drugs: Immune Checkpoint Agents in Acute Leukemia. *Curr Drug Targets*. 2017;18(3):315–31.
5. Hajam IA, Dar PA, Shahnawaz I, Jaume JC, Lee JH. Bacterial flagellin-a potent immunomodulatory agent. *Exp Mol Med*. 2017;49(9):e373.
6. Fu C, Jiang A. Dendritic Cells and CD8 T Cell Immunity in Tumor Microenvironment. *Front Immunol*. 2018;9:3059.
7. Coley WB. The Treatment of Inoperable Sarcoma by Bacterial Toxins (the Mixed Toxins of the *Streptococcus erysipelas* and the *Bacillus prodigiosus*). *Proc R Soc Med*. 1910;3(Surg Sect):1–48.
8. Hoption Cann SA, van Netten JP, van Netten C. Dr William Coley and tumour regression: a place in history or in the future. *Postgrad Med J*. 2003;79(938):672–80.
9. Forbes NS. Engineering the perfect (bacterial) cancer therapy. *Nat Rev Cancer*. 2010;10(11):785–94.
10. Hernandez-Luna MA, Luria-Perez R. Cancer Immunotherapy: Priming the Host Immune Response with Live Attenuated *Salmonella enterica*. *J Immunol Res*. 2018;2018:2984247.
11. Toley BJ, Forbes NS. Motility is critical for effective distribution and accumulation of bacteria in tumor tissue. *Integrative Biology*. 2012;4(2):165–76.
12. Clairmont C, Lee KC, Pike J, Ittensohn M, Low KB, Pawelek J, et al. Biodistribution and genetic stability of the novel antitumor agent VNP20009, a genetically modified strain of *Salmonella typhimurium*. *The Journal of infectious diseases*. 2000;181(6):1996–2002.
13. Thamm DH, Kurzman ID, King I, Li Z, Sznol M, Dubielzig RR, et al. Systemic administration of an attenuated, tumor-targeting *Salmonella typhimurium* to dogs with spontaneous neoplasia: phase I evaluation. *Clin Cancer Res*. 2005;11(13):4827–34.
14. Luo X, Li Z, Lin S, Le T, Ittensohn M, Bermudes D, et al. Antitumor effect of VNP20009, an attenuated *Salmonella*, in murine tumor models. *Oncol Res*. 2001;12(11–12):501–8.
15. Chorobik P, Czaplicki D, Ossysek K, Bereta J. *Salmonella* and cancer: from pathogens to therapeutics. *Acta Biochim Pol*. 2013;60(3):285–97.
16. Zhou S, Zhao Z, Lin Y, Gong S, Li F, Pan J, et al. Suppression of pancreatic ductal adenocarcinoma growth by intratumoral delivery of attenuated *Salmonella typhimurium* using a dual fluorescent live tracking system. *Cancer Biol Ther*. 2016;17(7):732–40.
17. Toso JF, Gill VJ, Hwu P, Marincola FM, Restifo NP, Schwartzentruber DJ, et al. Phase I study of the intravenous administration of attenuated *Salmonella typhimurium* to patients with metastatic melanoma. *Journal of clinical oncology: official journal of the American Society of Clinical Oncology*. 2002;20(1):142–52.
18. Heimann DM, Rosenberg SA. Continuous intravenous administration of live genetically modified *salmonella typhimurium* in patients with metastatic melanoma. *J Immunother*. 2003;26(2):179–80.
19. Liu Y, Cheng H, Gao S, Lu X, He F, Hu L, et al. Reprogramming of MLL-AF9 leukemia cells into pluripotent stem cells. *Leukemia*. 2014;28(5):1071–80.

20. Kazmierczak M, Szczepaniak A, Czyz A, Rupa-Matysek J, Komarnicki M. Spontaneous hematological remission of acute myeloid leukemia. *Contemp Oncol (Pozn)*. 2014;18(1):67–9.
21. Vachhani P, Mendler JH, Evans A, Deeb G, Starostik P, Wallace PK, et al. Spontaneous Remission in an Older Patient with Relapsed FLT3 ITD Mutant AML. *Case Rep Hematol*. 2016;2016:1259759.
22. Maywald O, Buchheidt D, Bergmann J, Schoch C, Ludwig WD, Reiter A, et al. Spontaneous remission in adult acute myeloid leukemia in association with systemic bacterial infection-case report and review of the literature. *Ann Hematol*. 2004;83(3):189–94.
23. Muller CI, Trepel M, Kunzmann R, Lais A, Engelhardt R, Lubbert M. Hematologic and molecular spontaneous remission following sepsis in acute monoblastic leukemia with translocation (9;11): a case report and review of the literature. *Eur J Haematol*. 2004;73(1):62–6.
24. Theys J, Pennington O, Dubois L, Anlezark G, Vaughan T, Mengesha A, et al. Repeated cycles of Clostridium-directed enzyme prodrug therapy result in sustained antitumour effects in vivo. *Br J Cancer*. 2006;95(9):1212–9.
25. Gupta A, Le A, Belinka BA, Kachlany SC. In vitro synergism between LFA-1 targeting leukotoxin (Leukothera) and standard chemotherapeutic agents in leukemia cells. *Leuk Res*. 2011;35(11):1498–505.
26. Bu S, Xie Q, Chang W, Huo X, Chen F, Ma X. LukS-PV induces mitochondrial-mediated apoptosis and G0/G1 cell cycle arrest in human acute myeloid leukemia THP-1 cells. *Int J Biochem Cell Biol*. 2013;45(8):1531–7.
27. Nagarsheth N, Wicha MS, Zou W. Chemokines in the cancer microenvironment and their relevance in cancer immunotherapy. *Nat Rev Immunol*. 2017;17(9):559–72.
28. Zhou YQ, Gao HY, Guan XH, Yuan X, Fang GG, Chen Y, et al. Chemokines and Their Receptors: Potential Therapeutic Targets for Bone Cancer Pain. *Curr Pharm Des*. 2015;21(34):5029–33.
29. Liu M, Guo S, Stiles JK. The emerging role of CXCL10 in cancer (Review). *Oncol Lett*. 2011;2(4):583–9.
30. Shimasaki N, Jain A, Campana D. NK cells for cancer immunotherapy. *Nat Rev Drug Discov*. 2020.
31. Gajewski TF, Schreiber H, Fu YX. Innate and adaptive immune cells in the tumor microenvironment. *Nat Immunol*. 2013;14(10):1014–22.
32. Vendrell A, Gravisaco MJ, Pasetti MF, Croci M, Colombo L, Rodriguez C, et al. A novel Salmonella Typhi-based immunotherapy promotes tumor killing via an antitumor Th1-type cellular immune response and neutrophil activation in a mouse model of breast cancer. *Vaccine*. 2011;29(4):728–36.

## Figures

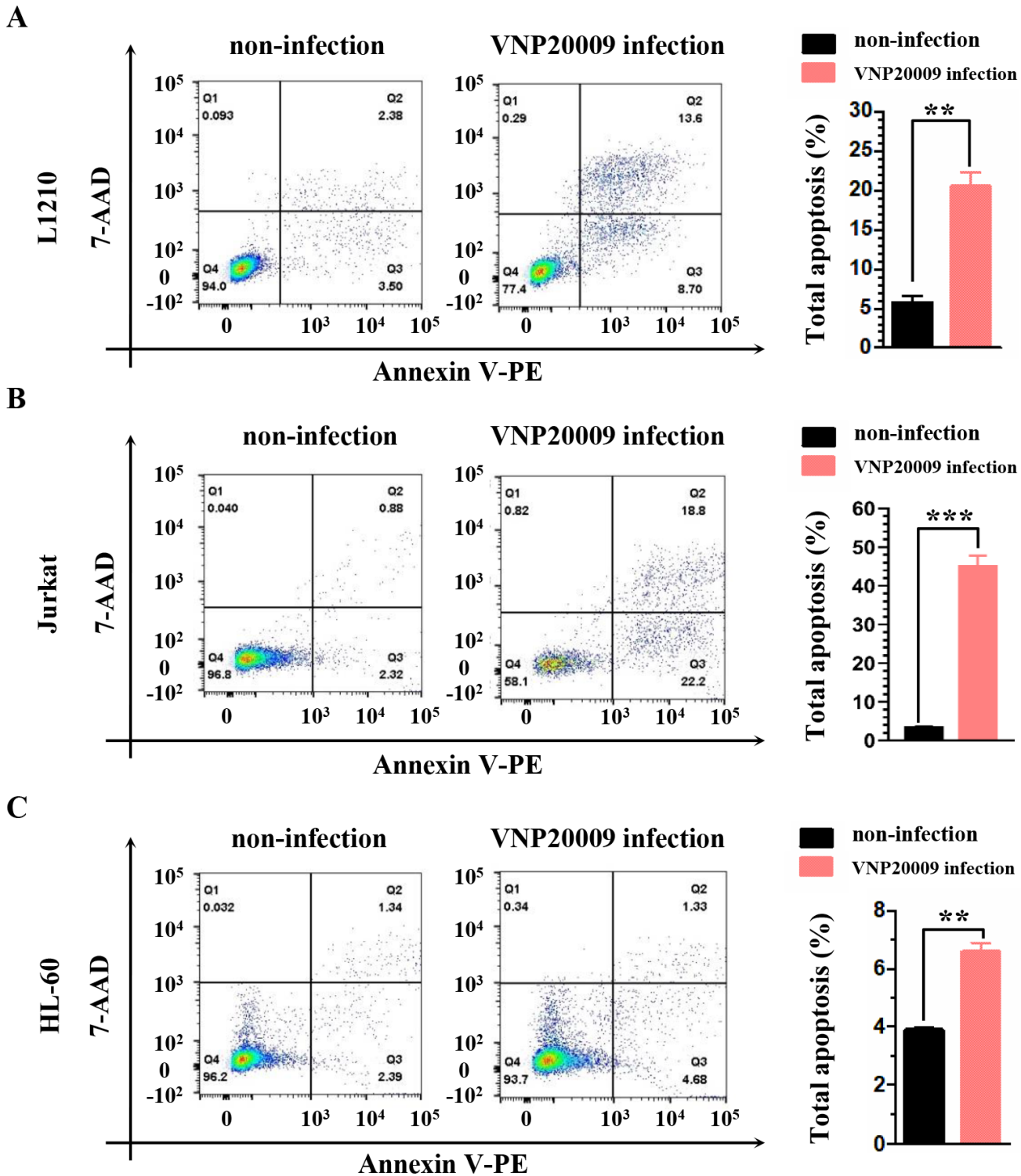


**Figure 1**

Induction of apoptosis of acute leukemia cells by VNP20009 treatment in vitro. Representative flow cytometry graphs of (A) L1210 cells, (B) Jurkat cells and (C) HL-60 cells after co-culture with PBS (non-infection) or VNP20009 (VNP20009 infection) for 48h. The numbers in the upper left quadrant (Q1), upper right quadrant (Q2), lower left quadrant (Q4) and lower right quadrant (Q3) represent the percentages of dead cells (Annexin V-PE-/7AAD+), late apoptotic cells (Annexin V-PE+/7AAD+), live cells

(Annexin V-PE-/7AAD-) and early apoptotic cells (Annexin V-PE+/7AAD-), respectively. The percentage of total apoptosis is the sum percentages of the late and early apoptosis. Statistical data are displayed in the right panel (n=3, biological replication). Statistical results were obtained by the two-tailed unpaired Student's t-test. \*P < 0.05, \*\*P < 0.01, \*\*\*P < 0.001. All data are expressed as mean  $\pm$  SEM.

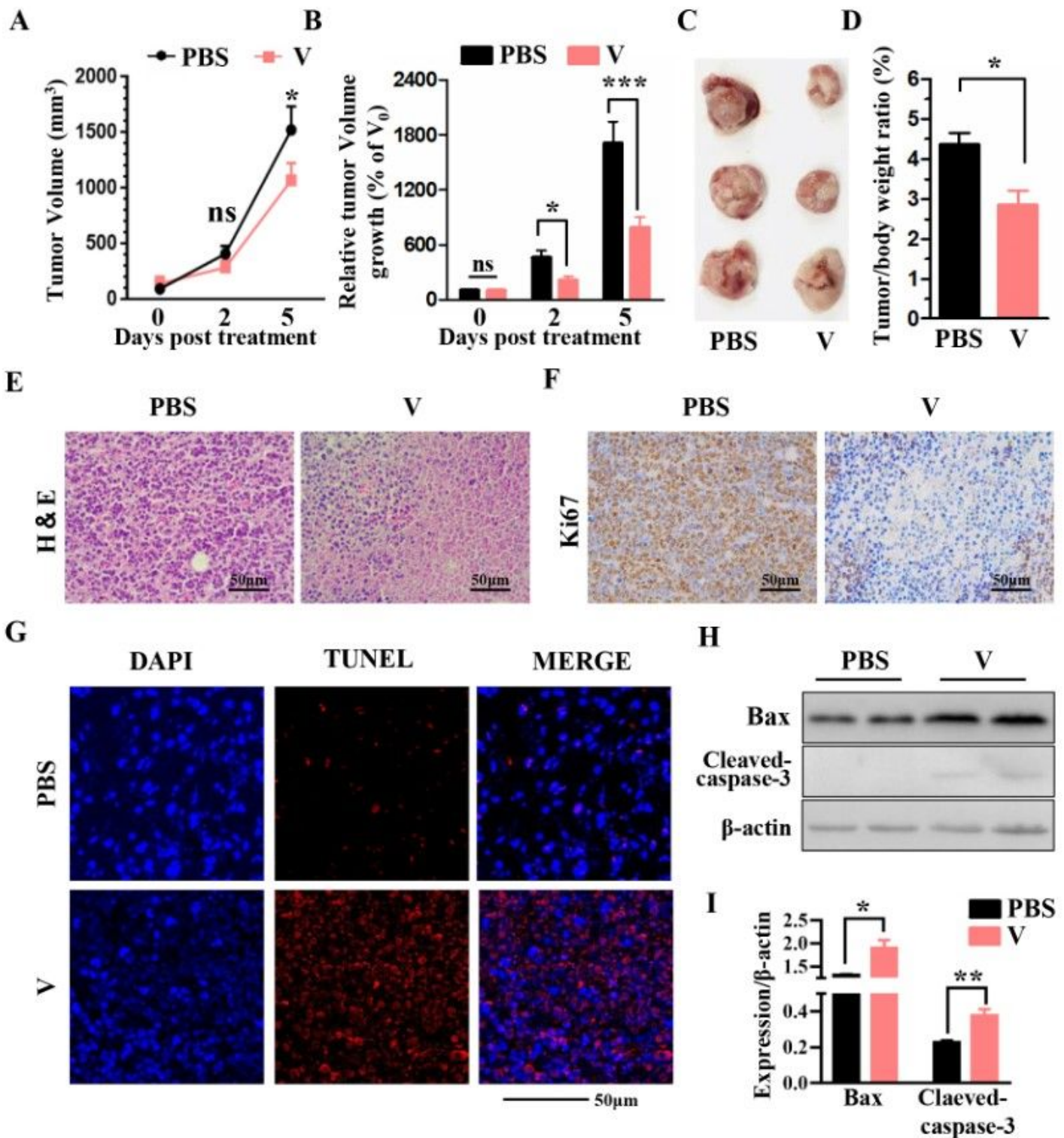
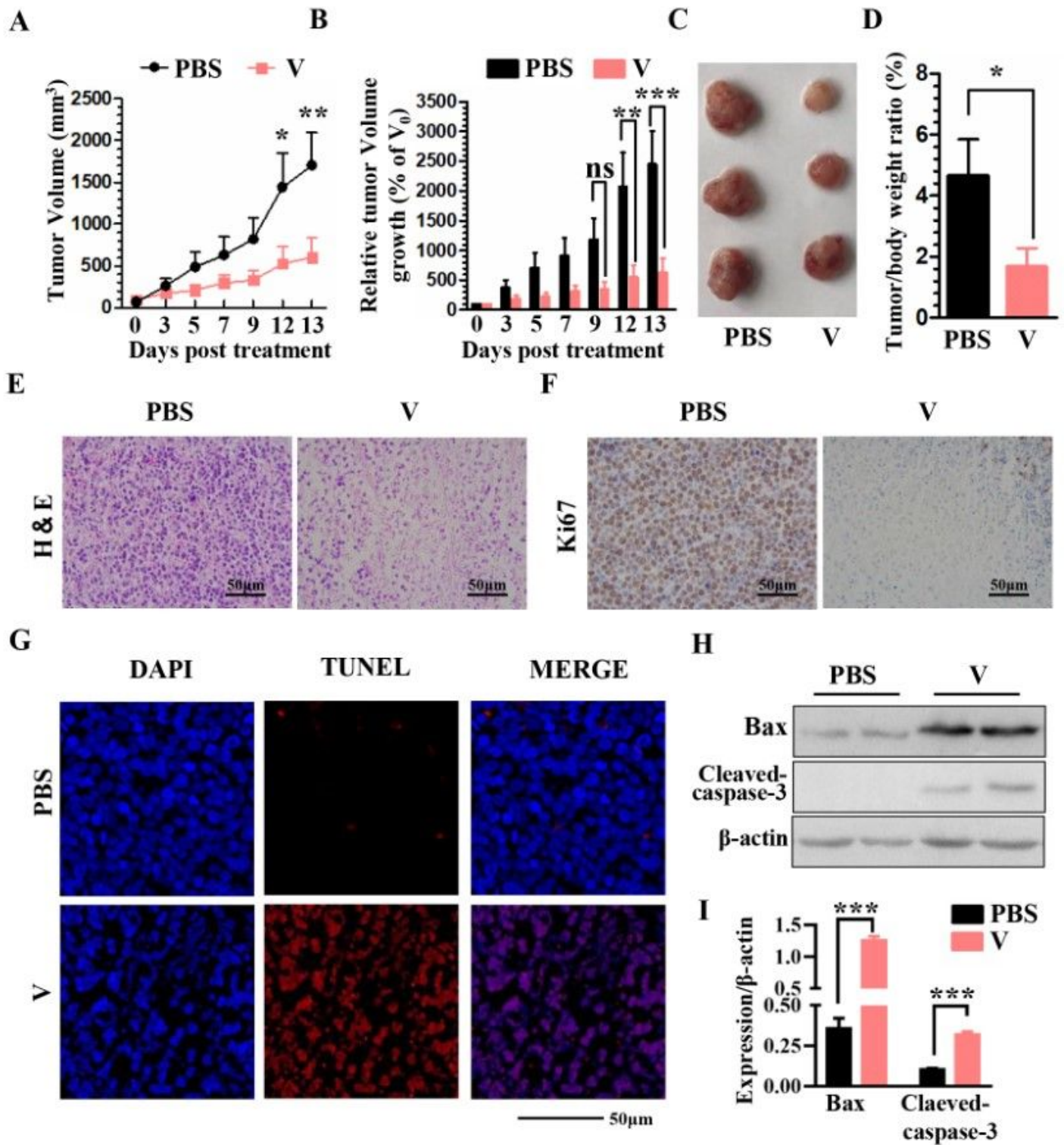


Figure 3

Suppression of L1210 subcutaneous tumor growth by VNP20009 in vivo. After tumor establishment, mice received a single intratumoral injection of PBS or VNP20009 ( $2 \times 10^6$  CFU/mouse,  $n = 6$ ). V is abbreviations for VNP20009. (A) The curve for tumor growth in inoculated nude mice. (B) The related tumor volume growth is expressed as % of  $V_0$  (initial therapeutic volume). (C) Tumor tissues were dissected and photographed at the end of treatment. (D) Tumors were weighed and tumor/body weight was calculated. (E) Representative microphotographs of H&E staining of tumor paraffin sections. (F) Representative immune-histochemical microphotographs of Ki-67-stained tumor paraffin sections. (G) Representative microphotographs of TUNEL-stained tumor paraffin sections. (H) Western blot analyses of Bax and cleaved-caspase-3 in L1210 tumors. (I) Bax and cleaved-caspase-3 were quantified and compared,  $n = 4$  mice per group. Scale bars,  $50 \mu\text{m}$ . \* $P < 0.05$ , \*\* $P < 0.01$ , \*\*\* $P < 0.001$ . All data are expressed as mean  $\pm$  SEM.



**Figure 5**

Suppression of HL-60 subcutaneous tumor growth by VNP20009 in vivo. After tumor establishment, mice received a single intratumoral injection of PBS or VNP20009 ( $2 \times 10^6$  CFU/mouse,  $n = 5$ ). V is abbreviations for VNP20009. (A) The curve for tumor growth in inoculated nude mice. (B) The related tumor volume growth is expressed as % of  $V_0$  (initial therapeutic volume). (C) Tumor tissues were dissected and photographed at the end of treatment. (D) Tumors were weighed and tumor/body weight

ratios were calculated. (E) Representative microphotographs of H&E staining of tumor paraffin sections. (F) Representative immune-histochemical microphotographs of Ki-67-stained tumor paraffin sections. (G) Representative microphotographs of TUNEL-stained tumor paraffin sections. (H) Western blot analyses of Bax and cleaved-caspase-3 in HL-60 tumors. (I) Bax and cleaved-caspase-3 were quantified and compared,  $n = 4$  mice per group. Scale bars, 50  $\mu\text{m}$ . \* $P < 0.05$ , \*\* $P < 0.01$ , \*\*\* $P < 0.001$ . All data are expressed as mean  $\pm$  SEM.

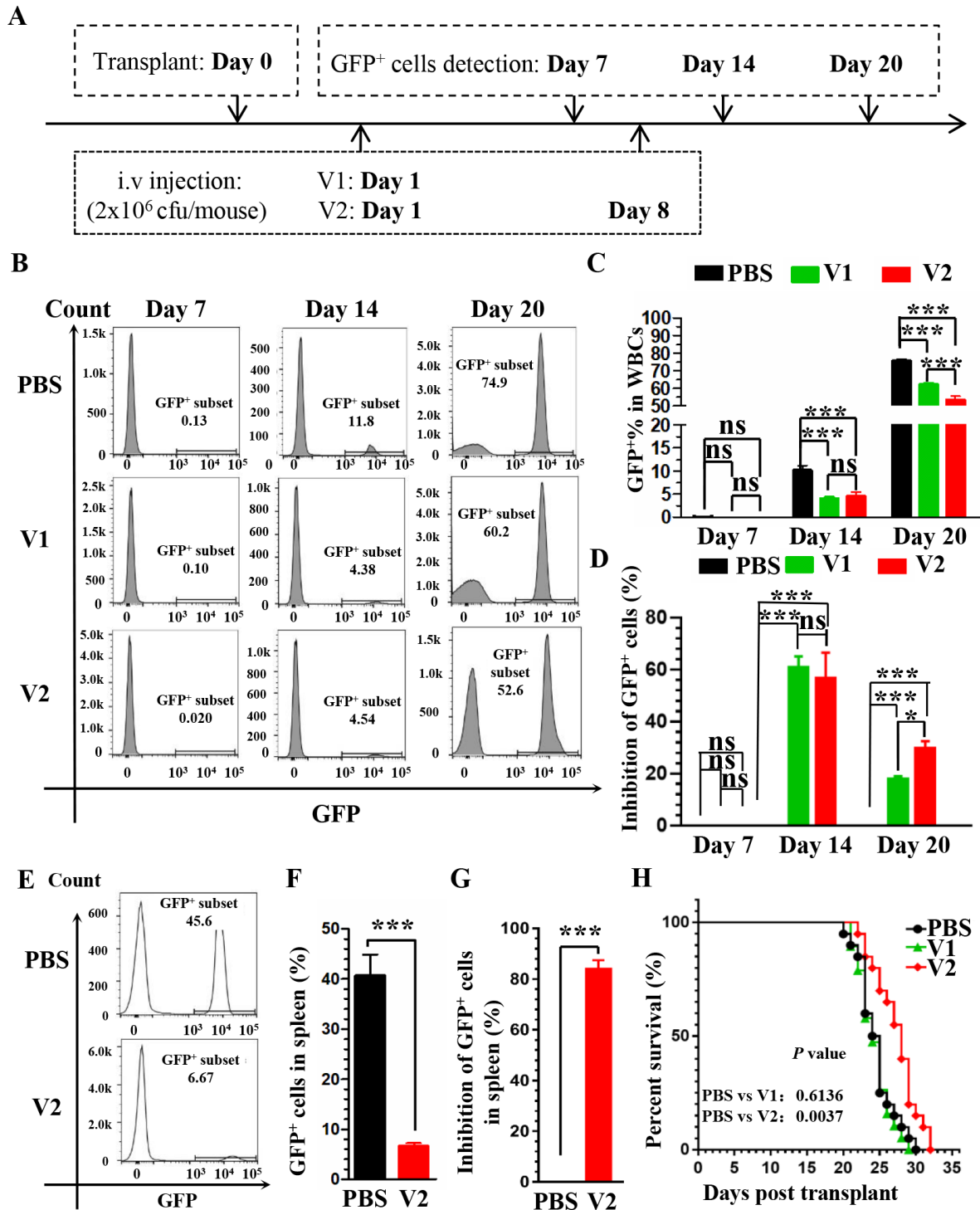
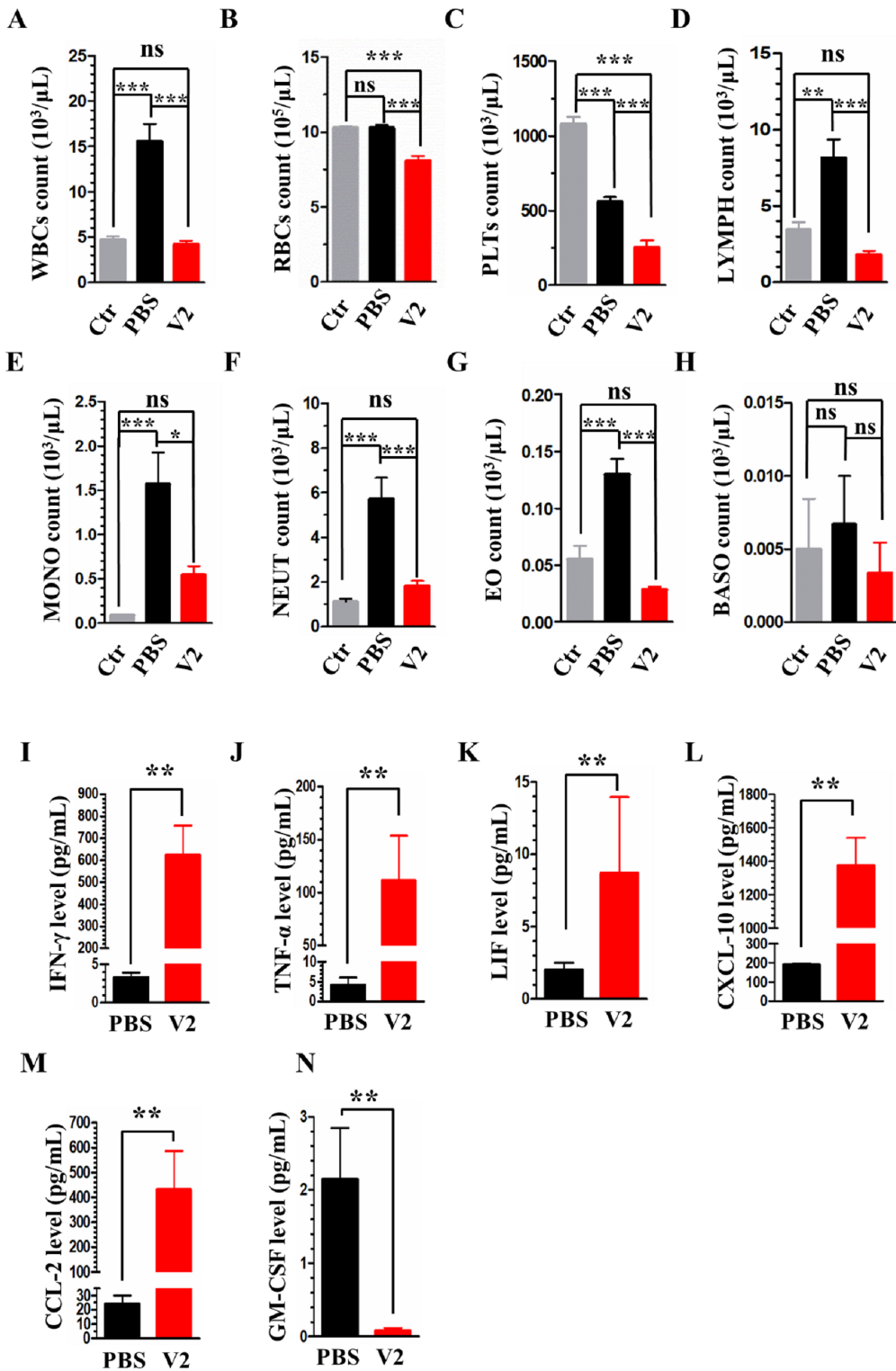


Figure 7

Therapeutic effects of VNP20009 on MLL-AF9-induced acute myeloid leukemia mice in vivo. The next day after mouse AML bone marrow cells were transplanted, mice received one (on day 1) or two (on day 1 and day 8) tail vein injections of PBS or VNP20009 ( $2 \times 10^6$  CFU/mouse, one dose: V1, two doses: V2). (A) The treatment and detection schedule. (B) Representative flow cytometry histograms of GFP+ AML cells in WBCs of mice on day 7, day 14, and day 20. (C) Quantification of the GFP+ AML cells in WBCs of mice on day 7, day 14, and day 20. (D) Inhibitory effects are expressed as % of the PBS control,  $n = 6$ . (E) Representative flow cytometry histograms of GFP+ AML cells in spleen of mice on day 14. (F) Quantification of the GFP+ AML cells in spleen of mice on day 14. (G) Inhibitory effects are expressed as % of the PBS control,  $n = 6$ . (H) The statistical analysis of survival rate of mice,  $P < 0.01$ , log-rank (Mantel-Cox) test,  $n = 19$ . \* $P < 0.05$ , \*\* $P < 0.01$ , \*\*\* $P < 0.001$ . All data are expressed as mean  $\pm$  SEM.



**Figure 9**

VNP20009 restores the counts of WBCs and its subtypes to near-normal levels, and affected the secretion of cytokines and chemokines in the VNP20009-treated AML mice. The counts of (A) WBCs, (B) RBCs, (C) PLTs, (D) LYMPHs, (E) MONOs, (F) NEUTs, (G) EOs and (H) BASOs in PB of MLL-AF9-induced acute myeloid leukemia mice on day 14. (Tail vein injection,  $2 \times 10^6$  CFU/mouse,  $n = 6$ ). The serum levels of (I) IFN- $\gamma$ , (J) TNF- $\alpha$ , (K) LIF, (L) CXCL-10, (M) CCL-2 and (N) GM-CSF in MLL-AF9-induced acute myeloid

leukemia mice on day 14. Ctr, control mice that raised normally; PBS, PBS-treated AML mice; V2, AML mice treated with two injections of VNP20009 (Tail vein injection,  $2 \times 10^6$  CFU/mouse,  $n = 3$ ). \* $P < 0.05$ , \*\* $P < 0.01$ , \*\*\* $P < 0.001$ . All data are expressed as mean  $\pm$  SEM.

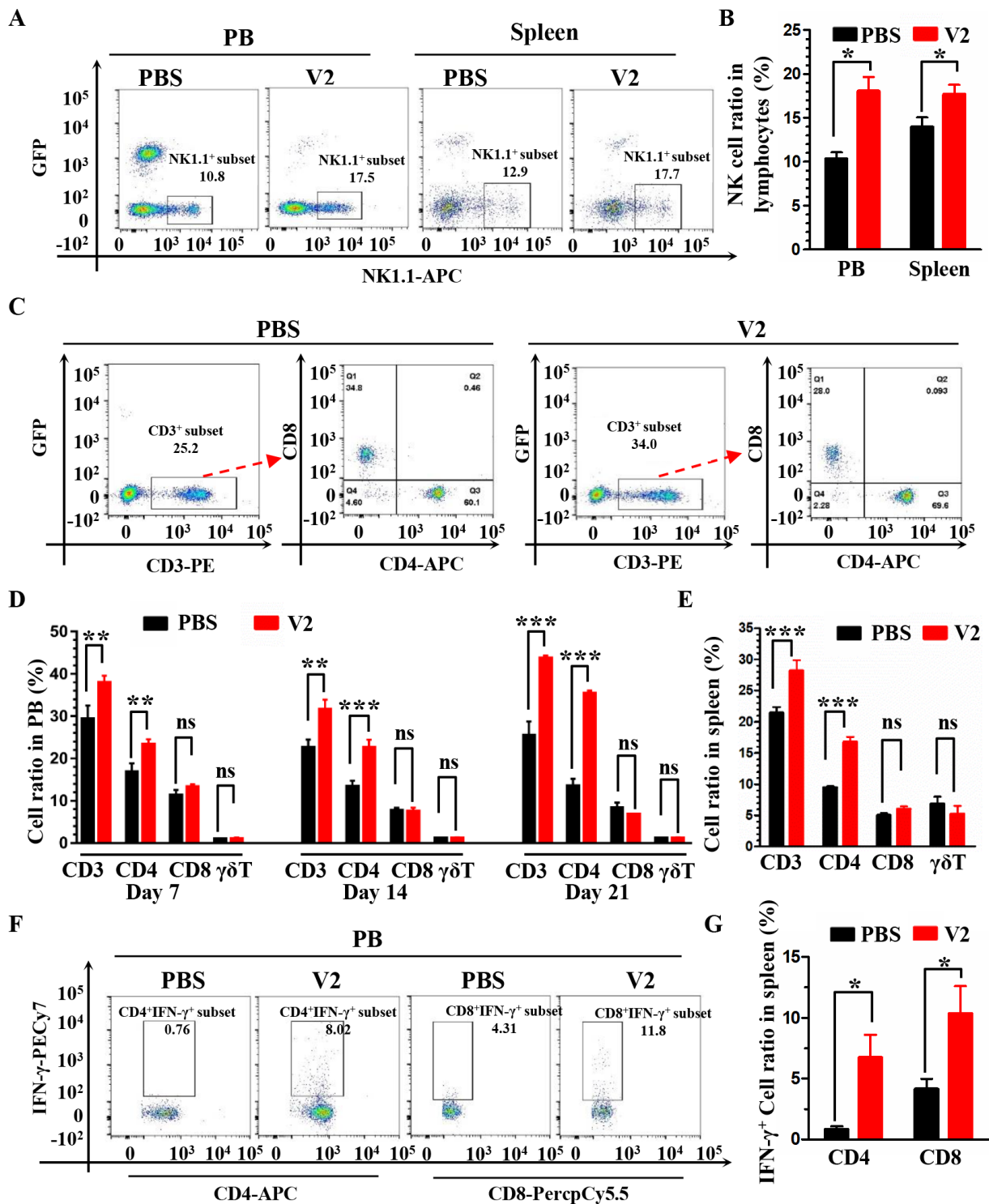


**Figure 11**

VNP20009 stimulates the native and adaptive immune cells in PB and spleen of MLL-AF9-induced acute myeloid leukemia mice. (A) Representative flow cytometry data of the NK+ cells in lymphocytes in PB and

spleen of mice on day 14. (B) Quantification of the NK+ cells in lymphocytes in PB and spleen of mice on day 14. (C) Representative flow cytometry data of the percentage of CD3+ gated on lymphocytes, then CD4+, CD8+ and  $\gamma\delta$ T (CD4- CD8-) cells gated on CD3+ cells in PB and spleen. The numbers in the upper left quadrant (Q1), lower left quadrant (Q4) and lower right quadrant (Q3) represent the percentages of CD8+ cells,  $\gamma\delta$ T cells and CD4+ cells, respectively. (D) Quantification of the CD3+, CD4+, CD8+ and  $\gamma\delta$ T cells in lymphocytes in PB of mice on day 7, day 14, and day 20. (E) Quantification of CD3+, CD4+, CD8+ and  $\gamma\delta$ T cells in lymphocytes in spleen of mice on day 14. (F) Representative flow cytometry histograms of the CD4+IFN- $\gamma$ + cells and CD8+IFN- $\gamma$ + cells in lymphocytes of spleen on day 14. (G) Quantification of the CD4+IFN- $\gamma$ + cells and CD8+IFN- $\gamma$ + cells in lymphocytes of spleen on day 14. \*P < 0.05, \*\*P < 0.01, \*\*\*P < 0.001. All data are expressed as mean  $\pm$  SEM. PBS, PBS-treated AML mice; V2, mice treated with two doses of VNP20009 (Tail vein injection,  $2 \times 10^6$  CFU/mouse, PB: n = 6, spleen: n = 3).

## Supplementary Files

This is a list of supplementary files associated with this preprint. Click to download.

- [SupplementaryFigures.pdf](#)
- [Fig.S1.tif](#)
- [Fig.S2.tif](#)
- [Fig.S1.tif](#)
- [Fig.S3.tif](#)
- [SupplementaryFigures.pdf](#)
- [Fig.S2.tif](#)
- [Fig.S3.tif](#)
- [Fig.S4.tif](#)
- [Fig.S4.tif](#)